9

Formation and Evolution Characteristics of Nano-Clusters (For Large-Scale Systems of 10^6 Liquid Metal Atoms)

Rang-su Liu*, Hai-rong Liu, Ze-an Tian,
Li-li Zhou and Qun-yi Zhou
Hunan University
China

1. Introduction

It is well known that the formation and evolution characteristics of clusters and nano-clusters have been studied, both experimentally and theoretically over the years. Many experimental works were carried out by using physical or chemical methods, such as ionic spray, thermal evaporation, chemical action deposition, and so on, to obtain some nice particles or clusters consisted of dozens to hundreds of atoms in special configurations (Echt et al, 1981; Knight et al, 1984; Harris et al, 1984; Schriver et al, 1990; Robles et al, 2002; Magudoapathy et al, 2001; Spiridis et al, 2001; Liu X H et al, 1998; Yamamoto et al, 2001; Bruhl R et al, 2004; Kostko et al, 2007; Alexander & Moshe, 2001) . The theoretical works were mainly carried out on diversified individual clusters configured by accumulating atoms according to some fixed pattern (Liu C. S. et al, 2001; Solov'yov et al, 2003; Doye & Meyer, 2005; Li H. & Pederiva, 2003; Ikeshoji et al, 1996; Wang L et al, 2002; Haberland et al., 2005; Joshi et al., 2006; Noya et al., 2007; Cabarcos et al., 1999; Orlando & James, 1999; Alfe, 2003). However, it is interesting that the similar clusters or aggregations have been found in some liquid metals during rapid solidification processes in our MD simulations (Liu R. S. et al., 1992a, 1992b, 1995, 2002, 2005a, 2005b, 2007a, 2007b, 2007c, 2009; Dong K. J. et al., 2003; Liu F. X. et al., 2009; Hou Z. Y. et al., 2009, 2010a, 2010b) and that it is also important for understanding in depth the solidification processes from liquid state to solid state. Furthermore, the formation and evolution characteristics of cluster configurations, especially the nano-cluster configurations, formed during solidification processes of liquid metals are still not well known up to now.

In this chapter, the main purpose is to further extended our previous MD simulation method (Liu R. S. et al., 2007a, 2007b, 2007c, 2009; Tian et al., 2008, 2009; Zhou et al., 2011) to study the large-sized systems consisting of 10^6 atoms of liquid metal Al and Na. Using the center-atom method, bond-type index method, and cluster-type index method (we proposed), the results have been analyzed and demonstrated that the larger simulation system can lead to a better understanding of the formation and evolution characteristics of the cluster configurations, especially the nano-clusters during solidification processes.

* Corresponding Author

2. Simulation conditions and methods

The molecular dynamics (MD) technique used here is based on canonical MD, and the simulation conditions are as follows: 10^6 atoms of metal Al, and the same for Na, are placed in a cubic box, respectively, and the systems run under periodic boundary conditions. The cubic box sizes are determined by both the number of atoms in each system and the mean volume of each atom at each given temperature, for these simulations the mean volumes are taken from the Ω-T curve as shown in Fig.5 of Ref (Qi D. W. & Wang S, 1991a) thus the box sizes would be changed with temperature. The motion equations are solved using leap-frog algorithm. The interacting inter-atomic potentials adopted here are the effective pair potential function of the generalized energy independent non-local model-pseudo-potential theory developed by Wang et al (Wang S. & Lai S. K., 1980; Li D. H., Li X. R. & Wang S., 1986). The effective pair potential function is

$$V(r) = \left(Z_{eff}^2 / r\right)\left[1 - \left(\frac{2}{\pi}\right)\int_o^\infty dqF(q)\sin(rq)/q\right] \tag{1}$$

where Z_{eff} and $F(q)$ are, respectively, the effective ionic valence and the normalized energy wave number characteristics, which were defined in detail in Refs. (Wang S. & Lai S. K., 1980; Li D. H., Li X. R. & Wang S., 1986). These pair potentials are cut off at 20 a.u (atom unit). The time step of simulation is chosen as 10^{-15}s.

The simulating calculations are performed for different metals respectively. For example, the simulation starts at 943K (the melting point (T_m) of Al is 933K), (for other metals at different temperatures). First of all, let the system run at the same temperature so as to reach an equilibrium liquid state determined by the energy change of system. Thereafter, the damped force method (Hoover et al., 1982; Evans, 1983) is employed to decrease the temperature of the system with the cooling rate of 1.00×10^{13} K/s to some given temperatures: 883, 833, 780, 730, 675, 625, 550, 500, 450, 400 and 350K. At each given temperature, the instantaneous spatial coordinates of each atom are recorded for analysis below. The bond-type index method of Honeycutt-Andersen (HA) (Honeycutt & Andersen, 1987), the center-atom method (Liu R. S., Li J. Y. & Zhou Q. Y., 1995) and the cluster-type index method (Dong et al., 2003; Liu R. S., et al., 2005a) are used to detect and analyze the bond-types and cluster-types of the related atoms in the system, and we go further to investigate the formation mechanisms and magic number characteristics of various clusters configurations formed during solidification processes at atomic level as follows.

3. Microstructure analysis

3.1 Pair distribution function

The pair distribution function $g(r)$ can be obtained by Fourier transformation of X-ray scattering structure factors $S_{\alpha\beta}(Q)$, and has been widely used to describe the structure characterization for liquid and amorphous metals. The validity of the simulation results can be verified by comparing the calculated pair distribution function $g(r)$ with the experimental results.

In this chapter, we inspect the g(r) curves of the system of Al at 943K and of the system of Na at 573K, 473K and 373K obtained from simulations and compare them with the experimental results obtained by Waseda (Waseda, 1980), as shown in corresponding

Figures 1 and 2 for Al and Na, respectively. From these Figures, it can be clearly seen that the simulation results are in good agreement with the experimental results. This means that the effective pair-potentials adopted here have successfully described the objective physical nature of these systems.

3.2 Bond-type index analysis

For deep understanding the formation and evolution mechanism of clusters in liquid metals, it is very important for us to know the concrete relationship of an atom with its near neighbors. Recently, the pair analysis technique has become an important method to describe and discern the concrete relationship of an atom with the near neighbors in liquid and amorphous systems. For a long time, the pair analysis technique, especially, the Honeycutt-Andersen (HA) bond-type indexes (Honeycutt & Andersen, 1987) have been successfully applied to describe and analyze the microstructure transitions in simulation systems, the details was shown in Refs (Liu R. S., et al., 2002; Dong K. J., et al., 2003). In this chapter, for the systems consisting of 10^6 atoms for Al and Na, various bond-types are also described by HA indexes, as shown in Table 1 and 2, respectively.

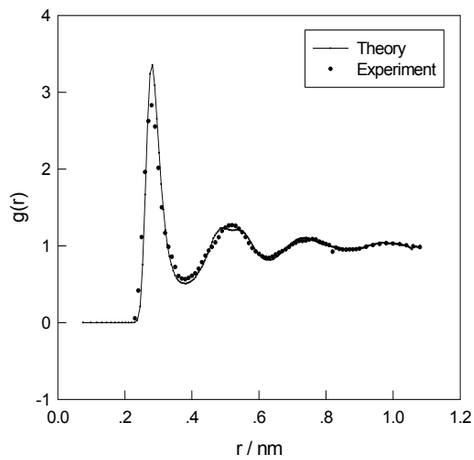

Fig. 1. Pair distribution function of liquid Al at 943K

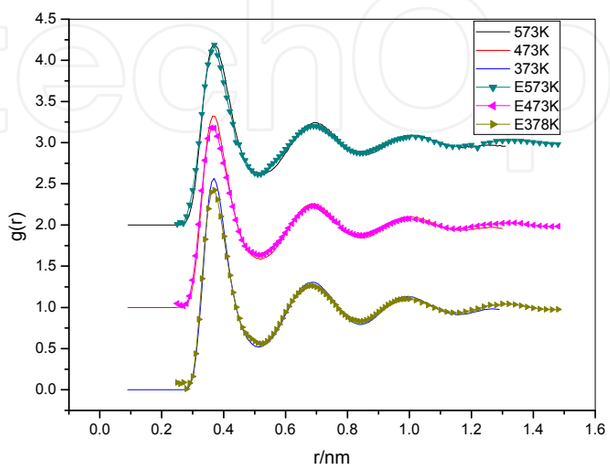

Fig. 2. Pair distribution function of liquid Na at 573K, 473K and 373K

From Table 1 and 2, it can be clearly seen that:

Firstly, the relative numbers of 1551 and 1541 bond-types, related to the icosahedral configurations and amorphous structures, play an important role: (1) For Al, they represent 14.3% and 13.2% at 943K, respectively, and the two bond-types represent 27.5% of the total bond-types. It is worth noting that these percentages change with the system temperature. At 350K, the proportion of 1551 bond-type increases remarkably with decreasing temperature, reaching 29.4% of the total, whilst the 1541 bond-type only increase slightly to 14.6% of the total; the sum of the 1551 and 1541 bond-types makes up 44.0% of all bond-types, indicating an increase of 16.5% from the corresponding proportion at 943K. (2) For Na, they represent 6.0% and 9.0% of all bond-types at 973K, respectively. While the sum of the 1551 and 1541 bond-types represents 45.8% of all bond-types, being increased about 30.8%. Highly interesting is that the relative numbers of 1551 bond-type is also increased remarkably with decreasing temperature, reaching 31.2% at 223K. From these results, it can be obviously seen that for the two systems, the 1551 bond-type plays a decisive role in the whole evolution process of microstructures.

For the relative numbers of the 1441, 1431, 1421 and 1422 bond-types related to the tetrahedral structures, the 1331, 1321, 1311 and 1301 bond-types related to the rhombohedral structures, and the 1661 bond-type related to hcp and bcc structures, are also similar to those obtained from previous works as above-mentioned.

Highly interesting is the 1771 bond-type, according to the definition of Honeycutt-Andersen bond-type indexes, it should possess seven-fold symmetry. It is well known that the seven-fold symmetry cannot exist in crystal solid state. However, in the Al system, although the relative number of 1771 bond-type is less than 0.1%, it still only exists in liquid and supercooled liquid states above 500K, and disappears in the solid state below 500K. This result just proves that the seven-fold symmetry cannot exist in crystal solid state, and further proves that the seven-fold symmetry also cannot exist in amorphous solid state. But for Na system, at 123K, it is still in the suppercooled liquid, so the 1771 bond-type can exist in it.

Temp (K)	Bond types and corresponding relative numbers (%)													
	1201	1211	1301	1311	1321	1331	1421	1422	1431	1441	1541	1551	1661	1771
943	1.6	1.5	1.0	7.2	7.2	0.7	3.3	7.1	21.2	4.4	13.2	14.3	4.5	0.1
883	1.5	1.4	0.9	6.9	7.0	0.6	3.2	6.9	21.3	4.5	13.5	15.2	4.7	0.1
833	1.3	1.3	0.9	6.5	6.7	0.6	3.1	6.8	21.3	4.5	13.7	16.3	4.9	0.1
780	1.2	1.2	0.8	6.1	6.4	0.5	3.0	6.5	21.3	4.6	13.9	17.7	5.1	0.1
730	1.1	1.1	0.7	5.7	6.1	0.5	2.9	6.3	21.2	4.6	14.1	19.1	5.4	0.1
675	0.9	0.9	0.7	5.2	5.7	0.5	2.8	6.0	21.1	4.6	14.3	20.9	5.6	0.1
625	0.9	0.9	0.6	5.1	5.6	0.4	2.7	5.9	21.1	4.5	14.5	22.0	5.7	0.1
550	0.9	0.9	0.6	4.8	5.4	0.4	2.6	5.7	21.0	4.3	14.6	24.0	5.7	0.1
500	0.8	0.9	0.6	4.7	5.4	0.3	2.5	5.6	21.1	4.1	14.6	25.3	5.6	0.1
450	0.8	0.9	0.5	4.5	5.3	0.3	2.4	5.4	21.0	3.9	14.6	26.8	5.6	0.0
400	0.7	0.9	0.5	4.3	5.2	0.3	2.3	5.3	20.9	3.8	14.6	28.2	5.6	0.0
350	0.7	0.9	0.5	4.2	5.2	0.3	2.2	5.1	20.8	3.6	14.6	29.4	5.5	0.0

Table 1. Relations of the number of various bond types (%)of Al with temperature (K).

	1201	1211	1301	1311	1321	1331	1421	1422	1431	1441	1541	1551	1661	1771
973	2.9	3.0	1.4	9.2	9.1	1.8	3.4	7.1	16.7	4.0	9.0	6.0	2.4	0.2
923	2.8	2.8	1.4	9.2	8.9	1.7	3.4	7.3	17.1	4.1	9.4	6.3	2.5	0.2
873	1.5	1.8	0.8	6.3	7.3	1.9	2.7	5.8	16.3	5.1	9.8	8.1	3.5	0.3
823	2.4	2.3	1.4	9.0	8.5	1.4	3.6	7.6	18.1	4.2	10.3	7.2	2.9	0.2
773	2.3	2.1	1.4	8.8	8.2	1.2	3.7	7.8	18.5	4.3	10.8	7.8	3.1	0.2
723	1.1	1.3	0.8	5.7	6.5	1.4	2.8	6.0	17.4	5.6	11.3	10.2	4.4	0.3
673	1.3	1.4	0.9	6.3	6.8	1.4	3.0	6.4	17.9	5.3	11.4	9.8	4.1	0.3
623	0.9	0.9	0.7	5.1	5.7	1.2	2.8	5.9	17.8	6.0	12.4	12.3	5.2	0.3
573	0.7	0.7	0.7	4.8	5.3	1.0	2.8	5.9	18.2	6.2	13.1	13.4	5.7	0.3
523	0.6	0.6	0.6	4.4	4.8	0.9	2.8	5.9	18.5	6.3	13.8	14.7	6.2	0.3
473	0.5	0.4	0.6	3.9	4.3	0.8	2.8	5.8	18.4	6.6	14.4	16.3	6.8	0.3
423	0.3	0.3	0.5	3.4	3.7	0.6	2.8	5.7	18.5	6.8	15.3	18.2	7.4	0.3
373	0.2	0.2	0.4	2.9	3.1	0.5	2.7	5.5	18.3	7.0	16.0	20.3	8.2	0.2
323	0.1	0.1	0.4	2.4	2.5	0.4	2.6	5.3	18.0	7.3	16.7	22.8	9.0	0.2
273	0.1	0.1	0.3	1.8	1.9	0.3	2.6	5.1	17.4	7.6	17.4	25.2	9.9	0.2
223	0.0	0.0	0.1	0.6	0.9	0.3	1.3	2.5	12.5	10.0	14.6	31.2	14.2	0.2
173	0.0	0.1	0.0	0.3	0.6	0.2	1.2	2.1	11.0	11.7	14.1	33.1	16.2	0.2
123	0.0	0.0	0.0	0.1	0.3	0.2	0.6	0.9	7.4	13.2	10.3	35.7	19.8	0.2

Table 2. Relations of the number of various bond types (%) of Na with temperature (K).

On the whole, these simulation results are rather close to those obtained in our previous works on different-sized liquid metal systems (Liu R. S., et al., 1998, 1999, 2005a, 2005b; Dong K. J., et al., 2003) ; that is to say, for different-sized liquid metal systems, the simulation results of relative numbers of corresponding bond-types are similar to each other, there being only a minor difference during solidification processes.

3.3 Cluster-type index analysis

As is well known that different combinations of bond-types can form different cluster configurations, however, the HA bond-type indices cannot be used to describe and discern different basic clusters formed by an atom with its nearest neighbors, especially, the different nano-clusters formed by some different basic clusters.

In order to differentiate the basic cluster and the polyhedron, we define the "basic cluster" as the smallest cluster composed of a core atom and its surrounding neighbor atoms. A larger cluster can be formed by continuous expansion, with a basic cluster as the core, according to a certain rule, or by combining several basic clusters together. A polyhedron is generally a hollow structure with no central atom as the core. This is the essential distinction of a polyhedron from a "basic cluster", such as the Bernal polyhedron. However, if a basic cluster is shaped as a certain polyhedron, for simplicity, we also call it a polyhedron cluster, such as icosahedral cluster, Bernal polyhedron cluster, and so on.

It is clear that the bond-types formed by each atom with its neighbor atoms in the system are different; the cluster configurations formed by these bond-types are also different. Even if some cluster configurations are formed by the same number of bond-types, their structures may still be completely different from each other, owing to a slight difference in bond-length or bond-angle. On this point, at present it is hard to use the bond-type index method

to describe clearly the cluster configurations of different types. In order to deal with this difficult matter, a cluster-type index method (CTIM) has been proposed (Liu R. S., et al., 1998, 1999, 2005a, 2005b; Dong K. J., et al., 2003) based on the HA indexes (Honeycutt & Andersen, 1987) and the work of Qi and Wang (Qi. & Wang, S., 1991b). According to the definition of basic cluster, four integers (N, n1441,n1551,n1661) also adopted to describe the basic clusters. The meaning of the four integers used in CTIM are as follows: the first integer represents the number of surrounding atoms which form a basic cluster with the central atom, i. e. the coordination number Z of the central atom; the second, third and fourth integers respectively represent the numbers of 1441, 1551 and 1661 bond-types, by which the surrounding atoms are connected with the central atom of the basic cluster. For example, (12 0 12 0) stands for an icosahedral cluster that is composed of 13 atoms: the central atom is connected to the surrounding atoms through twelve 1551 bond-types (i. e. the coordination number of the central atom Z=12); (13 1 10 2) stands for the defective polyhedron cluster composed of 14 atoms, the core atom is connected to the surrounding atoms with one 1441, ten 1551 and two 1661 bond-types (the coordination number Z=13). For ease of representation, some main basic clusters have been chosen from the simulation system of liquid metal Al as shown in Fig. 3.

By using the CTIM, the statistical numbers of various cluster-types at each given temperature have been obtained. For liquid metal Al, during the whole solidification process, there are 53 different basic cluster-types in the system, only 34 of them appearing more than 5 times at some temperatures are listed in Table 3. For liquid metal Na, there are 63 different basic cluster-types, of which only 34 main types are listed in Table 4 (only 17 types appearing more than 1000 times play a critical role).

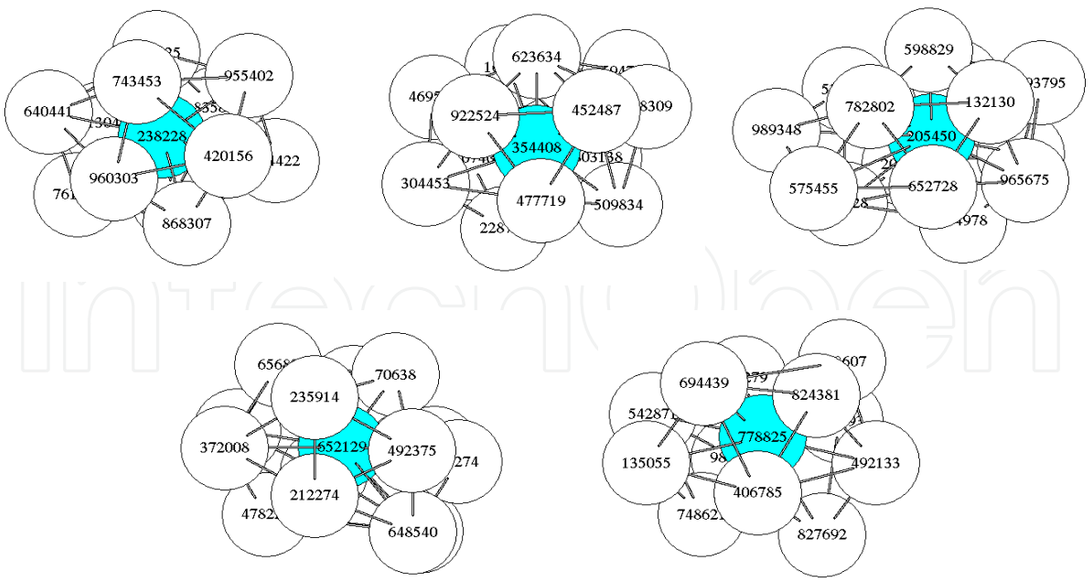

Fig. 3. Schematics of five main basic clusters at 350K: (a) icosahedral cluster（12 0 12 0） with central atom of 238228; (b) basic cluster（13 1 10 2）with central atom of 354408; (c) basic cluster（14 2 8 4）with central atom of 205450; (d) basic cluster（14 1 10 3）with central atom of 652129; (e) basic cluster（12 2 8 2）with central atom of 778825.

	Temperature (K) and the number of various cluster types											
Types of Cluster	943	883	833	780	730	675	625	550	500	450	400	350
(12 0 12 0)	2106	2819	3671	4867	6389	8698	10833	14857	18328	22216	26207	30153
(14 0 12 2)	183	210	253	368	447	564	751	881	1007	1189	1203	1360
(15 0 12 3)	78	68	103	126	165	208	262	358	410	391	478	472
(16 0 12 4)	8	19	17	27	31	40	34	46	55	63	74	83
(13 1 10 2)	1544	1919	2341	3078	3750	4870	5357	6522	7244	8125	8974	9417
(14 1 10 3)	427	536	684	894	1113	1366	1585	1881	2136	2382	2638	2892
(15 1 10 4)	172	213	285	366	452	568	647	845	899	1026	1092	1117
(16 1 10 5)	29	37	42	67	76	95	104	111	127	136	163	175
(17 1 10 6)	2	6	2	4	4	3	6	9	5	7	4	5
(10 2 8 0)	13	7	16	13	15	11	12	3	5	2	2	0
(11 2 8 1)	231	243	260	269	273	274	250	215	188	173	148	110
(12 2 8 2)	969	1066	1208	1440	1624	1865	1974	2117	2037	2067	2051	1956
(13 2 8 3)	396	452	548	585	740	882	933	960	1051	1029	999	1035
(14 2 8 4)	735	865	1014	1291	1632	1992	2194	2635	2758	2985	3286	3363
(15 2 8 5)	188	224	288	346	415	573	619	750	810	791	939	1023
(16 2 8 6)	23	26	52	59	56	75	86	94	77	102	110	122
(17 2 8 7)	0	3	2	6	5	5	7	8	4	0	2	3
(10 3 6 1)	3	6	5	2	1	5	4	3	1	1	1	0
(11 3 6 2)	41	36	38	33	29	23	19	19	20	13	5	8
(12 3 6 3)	288	260	301	359	375	345	322	253	276	199	174	140
(13 3 6 4)	914	1016	1191	1412	1651	1810	1951	1936	1884	1857	1782	1689
(14 3 6 5)	318	400	527	570	669	739	800	845	884	834	853	868
(15 3 6 6)	103	106	149	182	227	224	295	267	358	330	364	371
(16 3 6 7)	11	9	13	12	14	28	25	28	29	30	25	27
(11 4 4 3)	19	16	21	13	21	16	15	11	6	5	2	2
(12 4 4 4)	102	106	83	80	95	88	89	63	47	55	33	33
(13 4 4 5)	131	112	124	151	133	192	149	131	102	107	85	65
(14 4 4 6)	175	225	226	261	266	332	354	336	311	258	268	269
(15 4 4 7)	42	56	59	58	62	76	105	101	88	84	113	83
(16 4 4 8)	5	5	3	6	3	7	10	10	9	6	5	13
(12 5 2 5)	7	9	17	10	11	3	8	5	4	2	1	2
(13 5 2 6)	27	30	33	30	40	30	30	39	15	18	23	17
(15 5 2 8)	1	4	1	7	5	6	5	7	12	2	5	4
(14 6 0 8)	4	2	6	8	3	8	9	9	5	4	1	3
Total number of all clusters	9300	11117	13589	17006	20796	26029	29854	3 6365	41203	46498	52122	56885
Icosahedra expressed by (12 0 12 0) to total number (%)	22.65	25.36	27.01	28.62	30.72	33.42	36.29	40.85	44.48	47.78	50.28	53.01

Table 3. Variation of the number of clusters with temperature (K) for liquid metal Al.

Types of clusters	Temperatures (K) and the numbers of various cluster-types											
	973	873	773	673	573	523	473	423	373	323	273	223
(12 0 12 0)	16	39	58	92	320	536	749	1275	1888	2911	4475	7536
(14 0 12 2)	5	16	10	22	121	174	223	379	624	1000	1519	2879
(15 0 12 3)	1	6	11	14	54	68	118	185	284	431	673	1330
(16 0 12 4)	1	1	1	3	7	14	30	34	46	93	111	248
(13 1 10 2)	44	99	126	216	749	1089	1624	2357	3511	5270	7112	15029
(14 1 10 3)	10	28	39	109	289	414	662	923	1401	2076	2761	6360
(15 1 10 4)	7	19	7	52	181	241	373	533	812	1223	1760	4011
(16 1 10 5)	1	4	4	11	43	43	68	118	147	241	294	751
(10 2 8 0)	12	9	17	21	24	23	24	22	21	28	19	7
(11 2 8 1)	37	79	87	139	242	272	320	364	417	466	400	510
(12 2 8 2)	60	134	142	269	633	800	1073	1402	1946	2529	3031	5331
(13 2 8 3)	24	65	70	135	351	434	641	836	1098	1465	1792	4185
(14 2 8 4)	27	79	75	178	643	895	1355	1893	2805	4261	5808	14582
(15 2 8 5)	4	21	36	65	233	273	452	584	928	1310	1887	4979
(16 2 8 6)	3	4	2	16	36	60	86	83	145	207	217	662
(17 2 8 7)	0	1	0	1	4	2	6	9	14	5	16	34
(10 3 6 1)	11	16	11	18	23	31	19	19	15	11	13	5
(11 3 6 2)	16	42	41	53	73	49	82	66	89	62	69	57
(12 3 6 3)	44	127	119	184	408	525	649	743	793	946	1019	1653
(13 3 6 4)	76	163	184	365	1007	1350	1895	2538	3597	5027	6777	16150
(14 3 6 5)	13	62	71	159	420	510	816	1004	1565	2279	3050	8760
(15 3 6 6)	3	17	14	36	136	187	282	366	545	786	1055	3248
(16 3 6 7)	1	2	1	3	19	20	23	30	49	61	74	288
(11 4 4 3)	27	29	13	39	45	72	72	60	57	47	35	33
(12 4 4 4)	20	67	49	104	189	211	248	332	313	361	367	691
(13 4 4 5)	14	54	47	80	246	295	367	490	592	786	908	2240
(14 4 4 6)	11	36	43	78	289	420	575	781	1174	1751	2613	8125
(15 4 4 7)	2	8	5	19	61	75	114	157	240	347	511	1992
(16 4 4 8)	0	2	0	2	3	7	13	11	14	17	27	121
(12 5 2 5)	2	6	10	19	31	34	38	43	33	53	50	87
(13 5 2 6)	2	2	17	16	43	62	101	113	173	202	349	856
(15 5 2 8)	0	0	1	4	2	11	8	19	27	44	71	319
(16 5 2 9)	0	0	0	1	0	1	0	2	4	1	5	27
(14 6 0 8)	0	1	0	3	11	9	17	30	47	102	173	731
Total numbers of all clusters	494	1238	1311	2527	6936	9207	13123	17801	25414	36399	49041	113817
Icosahedrons expressed by (12 0 12 0) to total numbers(%)	3.23	3.15	4.42	3.64	4.61	5.82	5.71	7.16	7.43	7.99	9.13	6.6

Table 4. Variation of the number of clusters with temperatures (K) for liquid metal Na.

For liquid metal Al, from Table 3, however, it can be clearly seen that only 18 cluster-types appearing more than 100 times play a critical role in the solidification process. For convenience of discussion, we only show the variations of ten significant basic clusters with temperature in Figure 4(a) and (b). From Figure 4 (a), it is clear that among the most significant five basic clusters, the highest one is the icosahedral basic cluster expressed by (12 0 12 0), which increases rapidly as the temperature comes down. The number of basic cluster (12 0 12 0) climbs above 30,000 at 350K, and this cluster-type plays the most important role in the microstructure transitions during rapid solidification process. The second one is the basic cluster expressed by (13 1 10 2) and its number over 9400 at 350K. The number of the fifth cluster type expressed by (12 2 8 2) is over 1956 at 350K and still plays a certain role.

Figure 4 (b) presents that the numbers of basic clusters (14 0 12 2), (15 1 10 4), (13 2 8 3) and (15 2 8 5) all changed at about the same rate, except the basic cluster (13 3 6 4), and their numbers are in the range of 1023 - 1360 at 350K. Therefore, these clusters play only a secondary role.

However, as we go further to observe the Figures 4 (a), (b) and Table 3 carefully, it can be seen that the basic clusters (12 0 12 0) and (13 3 6 4) have almost a same turning point T_t in the range of 550-625K; in particular for cluster (13 3 6 4), T_t is a peak value point, it means that the cluster (13 3 6 4) plays an opposite role to the cluster (12 0 12 0) in the solidification process. Maybe just these cluster-types play a particular role, this turning point T_t is in agreement with the glass transition temperature T_g obtained by Liu et al (Liu R. S., Qi & Wang S., 1992; Wendt & Abraham, 1978; Zheng *et al*., 2002). On the other hand, this confirms that the glass transition temperature T_g can also be found by the turning point T_t in the relations of the numbers of main basic clusters with temperature. Therefore, it is possible to find a new method to determine the glass transition temperature T_g.

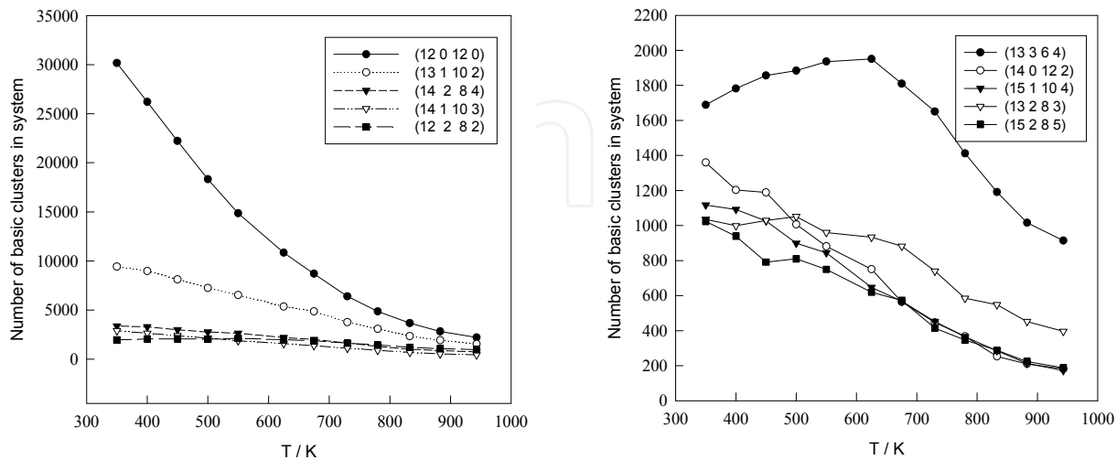

(a) (b)

Fig. 4. Variation of the numbers of the ten main basic clusters with temperatures for Al.

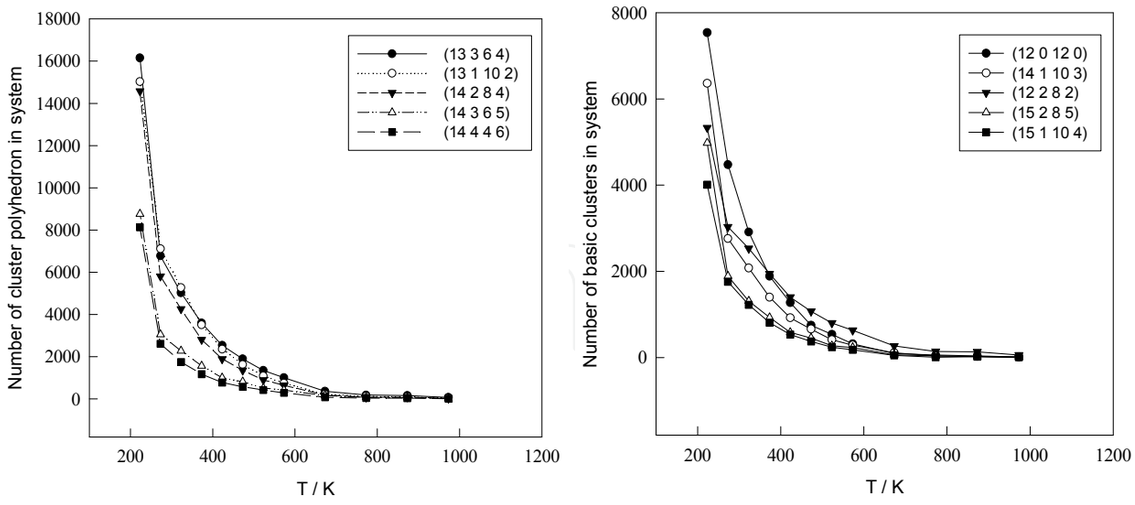

(a) (b)

Fig. 5. Relations of the numbers of 10 main basic clusters with temperature for Na.

It is worth noting that, from Table 3, it can be clearly seen that even at 943K, there are still a certain number of various basic clusters in the liquid state. That is to say, the liquid state discussed here is not an ideal liquid, as usually imagined, in which no cluster exist and each atom is free to diffuse. Furthermore, from our previous works for a small system consisting of 500 Al atoms, as shown in Fig.3 of Ref (Liu R. S., et al, 1999), it can be seen that even the temperature is increased up to 1800K ($\approx 2T_m$), the number of 1551 bond-type (which plays a leading role in microstructure transition of liquid metal Al) is still occupied 7.3 % of the total bond-types (and 16.5 % at 943K); thus some basic clusters formed mainly by 1551 bond-type would still be in the liquid system. If we want to get an ideal liquid state, the temperature should be increased higher and higher. In general, from the view point of microscopic structure, it is hard to completely reach the ideal case.

For liquid metal Na, for convenience of discussion, only the relations of the former 10 main basic clusters with temperature are shown in Fig.5. From Fig.5 (a), it can be clearly seen that the first 3 basic clusters (13 3 6 4), (13 1 10 2) and (14 2 8 4) are increased rapidly with decreasing temperature, and play almost the same important role in the microstructure transitions of liquid metal Na. While the basic cluster (12 0 12 0) has been ranked as the sixth one and only plays a secondary role; however, in the liquid metal Al, it is the first one and plays the most important role in the microstructure transitions (Liu R. S. et al., 2005a).

4. Formation and evolution of nano-clusters

4.1 Formation and description of nana-clusters

In this section, some nano-clusters have been described. They are composed of various kinds of smaller clusters, and their sizes and amounts are increased with temperature decreasing. Their configurations are very complex.

As above mentioned, we have defined the basic cluster as the smallest cluster composed of a core atom and its surrounding neighbor atoms. A larger cluster can be formed by

continuous expansion, with a basic cluster as the core, according to a certain rule, or by combining several basic clusters together.

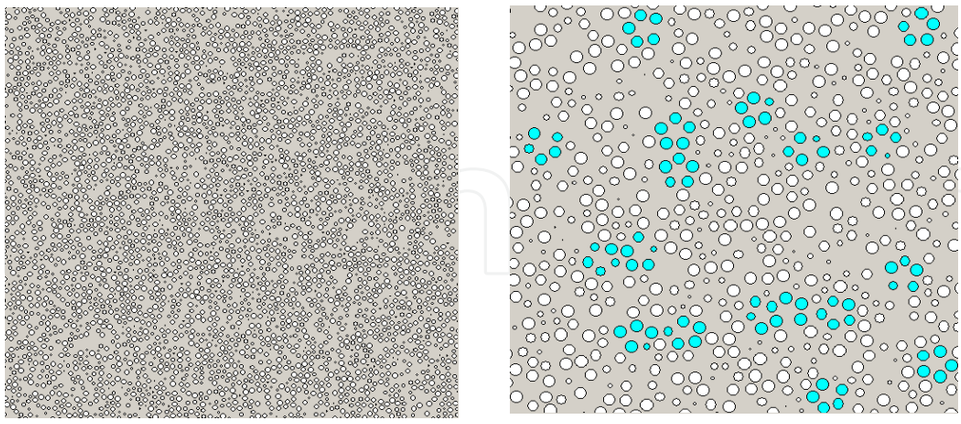

(a) (b)

Fig. 6. The 2D schematic of the whole system consisting of 1,000,000 atoms at 350K: (a) a part of (111) cross section×2 times ; (b) a part of (111) cross section ×5 times.

First of all, we display the whole schematic diagram of the 2D (111) cross section of the 1000000 atoms system of Al at 350 K, as shown in Fig.6(a) and (b), a part of (111) cross section × 2 times and a part of (111) cross section × 5 times, respectively. Fig.6(a), (b) show that the system has become amorphous state and formed two types of region: the dense region and the loose region. In the dense regions, some regular or distorted five-lateral patterns appear in Fig.6(b), which are just the cross sections of some icosahedron and their combining configurations. The loose regions are also of different sizes and shapes without apparent regulation and the atoms are randomly distributed there. The dense regions and the loose regions are also distributed randomly in the system; the inhomogeneous solid seems to be rather sponge-like with cavities (also commonly called "free volume") in different sizes and shapes.

It is clear that the microstructure of this system is hard to be described by the well-known model of "random hard sphere packing", since that model is too simple for describing amorphous metals. Figure 6, however, shows a typical amorphous picture, thus it is necessary to establish a new model to describe the complex structures of amorphous metals in the near future.

In these simulations, some larger clusters have been found. They are composed of various kinds of basic clusters and their sizes and numbers increase with temperature decreasing. Their configurations are very complex. For example, a larger cluster consisting of 68 atoms is composed of 10 basic clusters with central atoms (represented by gray circle) in Al system as shown in figure 7(a) , (b), displaying the whole atoms and the central atoms, respectively. From figures 7(a) and (b), it can be clearly seen that the larger cluster is formed by combining different medium-sized clusters, and each medium-sized cluster is also composed of some basic clusters that can be described by a set of indexes in the CTIM as shown in the caption. Interestingly, the larger clusters formed during rapid solidification processes of liquid metals Al and Na do not consist of multi-shell configurations

accumulated by atoms as obtained by gaseous deposition or ionic spray methods. However, the cluster configurations of Al formed by gaseous deposition have been verified by mass-spectrometer to be crystals or similar structures formed in octahedral shell structures (Martin, et al., 1992). Therefore, it can be concluded that different methods of preparing metallic materials would produce different cluster configurations. Figure 7 shows that the atoms contained in the larger clusters are labeled randomly, that is to say, the atoms in the system have been distributed homogeneously.

4.2 Evolution of nana-clusters

In order to display clearly the evolution characteristics of nano-clusters, it is necessary to trace the evolution processes of nano-clusters during rapid solidification processes. Adopting an inverse-evolving method, some tracking studies for the structural configurations of the nano-clusters have been performed. The evolution processes of the nano-clusters, at different temperatures, have been shown in Figures. It can be clearly seen that the central atoms of basic clusters of the nano-clusters are bonded with each other, some central atoms are multi-bonded, and others single-bonded.

In this simulation, some nano-clusters have been found. They are composed of various kinds of smaller clusters, and their size and amount are increased with temperature decreasing. Their configurations are very complex. For example, a nano-cluster consisting of 126 atoms are composed of 24 basic clusters with center atoms (represented by gray circle), as shown in Fig.8 (a), (b). It can be seen that the nano-cluster is produced by combining three different middle clusters, and each middle cluster composed of some basic clusters, and each basic cluster described by a set of indexes in CTIM.

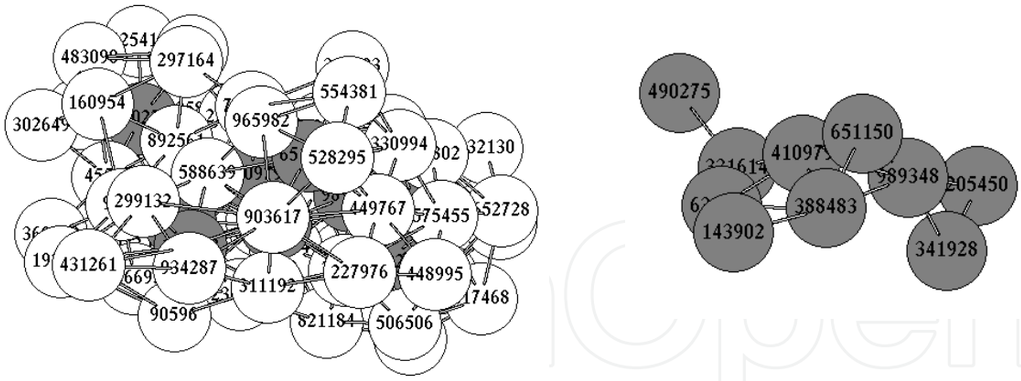

Fig. 7. Schematic diagram of a larger cluster consisting of 68 atoms within ten basic clusters with connecting bonds at 350 K (the gray spheres are the center atoms of basic clusters). The cluster is composed of 1 icosahedron (12 0 12 0), and basic clusters of 1 (16 0 12 4), 5 (13 1 10 2), 1 (14 1 10 3), 1 (14 2 8 4) and 1 (14 3 6 5). (a) displays all the atoms; (b) displays only the central atoms.

In order to display clearly the evolution characteristics of nano-clusters, it is necessary to trace the evolution processes of nano-clusters during rapid solidification processes. From our previous simulation results (Liu R S, et al., 1995, 2002), we have known that once an atom became the center of a cluster, it would possess certainly relative stability and

continuity (namely heredity). According to this feature, we can adopt the label of the central atom of a basic cluster to simplify the description of the nano-clusters, thus we can understand the whole evolution process of them more clearly. Adopting an inverse-evolving method, a tracking study for the structural configurations of this nano-cluster has been made.The evolution process of the nano-cluster, at different temperatures (for simplicity, we only select 2 different temperatures), has been shown in Fig.8(c),(d). It can be clearly seen that when the temperature is below 350K, the central atoms of 24 basic clusters of the nano-cluster are bonded with each other, some central atoms are multi-bonded, and others single-bonded. However, this is a very important characteristic for simplifying the research on the evolution processes and mechanisms of nano-clusters. With the increase of temperature, the maximal size of the original middle and small clusters decreases continuously. From the macro-viewpoint, such a degree of order is rather consistent with the statistical rules of thermodynamics. It can be clearly seen that this nano-cluster is also formed by connecting various middle and small clusters with different cluster-types or sizes, and different from that obtained by gaseous deposition, ionic spray and so on. It is well known that the latter is proved by mass-spectrometric analysis to be the nano-level crystal clusters formed by octahedron-shells configuration accumulated with an atom as the center (Joshi et al., 2006).

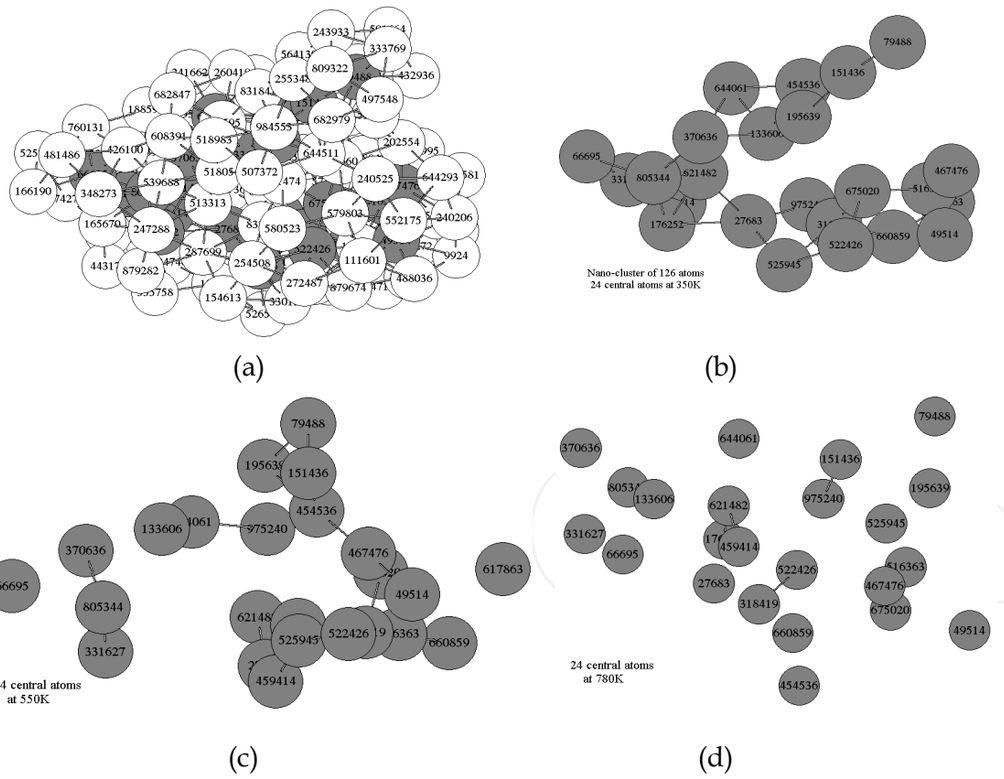

Fig. 8. Schematic figures of a nano-clusters consisting of 126 atoms within 24 basic clusters with connecting bonds at 350 K(the gray spheres are the center atoms of basic clusters). The cluster is composed of 7 icosahedron (12 0 12 0), and basic clusters of 1 (14 0 12 2), 5 (13 1 10 2), 3 (14 1 10 3), 3 (15 1 10 4), 1 (12 2 8 2), 2 (14 2 8 4), 1 (15 2 8 5) and 1 (15 3 6 6). (a) the whole atoms; (b) at 350K; (c) at 550K; (d) at 780K.

4.3 Size distribution and magic number sequence of nana-clusters

In order to investigate the size distribution characteristics of various clusters in the system, the relationship between the numbers of various clusters and their sizes (the numbers of atoms contained in each cluster) should be displayed clearly according to some statistical method. For convenience of discussion, we propose a new statistical method as follows.

Since a larger cluster can be described clearly by different basic clusters in the CTIM, all the clusters (from basic cluster to larger cluster) in the system can be classified according to the numbers of basic clusters contained in the larger cluster under consideration. Then, the clusters containing the same numbers of basic clusters can be further classified as a group. However, the clusters within a same group may not have the same number of atoms because the different basic clusters they contained would have different number of atoms. Thus there is a certain range of the numbers of atoms for a group of clusters, this can be clearly seen below.

Cluster consisting of 1 basic clusters		Cluster consisting of 2 basic clusters		Cluster consisting of 3 basic clusters		Cluster consisting of 4 basic clusters		Cluster consisting of 5 basic clusters	
Cluster size	Cluster number	Cluster size	Cluster number	Cluster size	Cluster number	Cluster size	Cluster number	Cluster size	Cluster number
Number of atom	943K 350K	Number of atom	943K350K	Number of atom	943K350K	Number of atom	943K350K	Number of atom	943K350K
11	13 0	17	1 0	23	9 210	26	0 7	30	0 2
12	245 55	18	6 4	24	19 204	27	0 27	31	0 6
13	**2254 10606**	**19**	167 **2761**	**25**	28 **647**	28	2 47	32	0 9
14	1912 3159	**20**	**269** 1432	26	53 551	29	4 130	33	1 23
15	998 1611	21	311 1370	**27**	**62 588**	30	10 128	34	3 46
16	300 433	22	202 730	28	43 451	31	8 212	35	0 69
17	39 37	23	86 273	29	32 202	32	9 210	36	4 69
18	0 1	24	46 56	30	21 106	**33**	10 **225**	37	1 105
		25	13 15	31	3 38	34	7 194	**38**	**7 118**
		26	2 1	32	4 15	**35**	**15** 126	39	6 106
				33	1 3	36	3 83	40	0 110
						37	4 27	41	2 69
						38	1 17	42	1 46
						39	1 7	43	1 27
						40	0 1	44	1 15
						41	0 1	45	0 7
						42	0 2	46	0 5
								47	0 2

(continued)

Cluster consisting of 6 basic clusters		Cluster consisting of 7 basic clusters		Cluster consisting of 8 basic clusters		Cluster consisting of 9 basic clusters		Cluster consisting of 10 basicclusters	
Cluster size	Cluster number	Cluster size	Cluster number	Cluster size	Cluster number	Cluster size	Cluster number	Cluster size	Cluster number
Number of atom	943K 350K	Number of atom	943K350K	Number of atom	943K350K	Number of atom	943K350K	Number of atom	943K350K
35	0 2	37	0 1	44	0 1	46	0 1	56	0 2
36	0 3	38	0 0	45	0 0	47	0 0	57	0 1
37	0 7	39	0 0	46	0 1	48	0 0	58	0 1
38	1 7	40	0 0	47	0 2	49	0 2	59	0 1
39	2 16	41	0 4	48	0 4	50	0 0	60	0 2
40	0 34	42	1 3	49	0 3	51	0 0	61	0 1
41	1 36	43	1 8	50	1 8	52	0 3	**62**	0 **7**
42	2 **54**	44	0 13	51	0 12	53	0 0	63	0 5
43	0 51	45	0 12	52	0 11	54	0 4	64	0 4
44	2 33	46	0 19	53	0 13	55	0 6	65	0 3
45	0 51	47	0 23	54	0 16	56	0 3	66	0 4
46	0 45	**48**	2 **33**	55	0 17	57	0 7	**67**	0 **9**
47	0 21	49	1 17	56	0 16	58	0 5	68	0 6
48	0 27	50	0 27	57	0 10	59	0 5	69	0 6
49	0 12	51	0 29	58	0 13	60	0 7	70	0 2
50	0 9	52	0 20	**59**	0 **22**	61	0 9	71	0 0
51	0 8	53	0 18	60	0 11	62	0 3	72	0 1
52	0 1	54	0 12	61	0 6	63	0 7	73	0 1
53	0 1	55	0 6	62	0 3	64	0 2	74	0 2
		56	1 4	63	0 0	**65**	0 **14**	75	0 1
		57	0 4	64	0 1	66	0 4	76	0 0
		58	0 3	65	0 1	67	0 1	77	0 0
		59	0 1	66	0 1	68	0 6	78	0 1
						69	0 1		
						70	0 2		

Table 5. Relations of the number of clusters consisting of 1-10 basic clusters with the cluster size (number of atoms included) for liquid metal Al.

4.3.1 Magic number sequence of nana-clusters for liquid metal Al

For liquid metal Al, for simplicity, we only analyze ten groups in the system in turn by the numbers of basic clusters contained in each group for two cases of liquid state at 943K and solid state at 350K, as shown in Table 5. From Table 5, it can be clearly seen that there is a peak value (maximum) of the numbers of clusters for each group and this is shown with a short underline in the table. As we compare this peak value with the abundance usually used in the research of cluster configurations, it is found that the two concepts are

completely consistent with each other. As we display the relations of the numbers of clusters formed in system with the size (the number of atoms contained in them) of these clusters, it is further found that the positions of the peak value points of the numbers of clusters also correspond to the magic number points. It is also clearly seen that the numbers of clusters at 943K are much less than those for the same group level at 350K for the former five group levels and there are few or almost none for the latter five group levels; and the front five peak value positions of clusters at 943K are not all consistent with those at 350K, for convenience of discussion for magic numbers, we only show the simulation results at 350K in figure 9.

It is clear from figure 9 that the quantity of various clusters is sensitive to the size of a cluster, and the magic numbers do exist. In the solid state at 350K, the total magic number sequence of all groups are in turn as 13, 19, 25, 27, 31, 33, 38, 40, 42, 45, 48, 51, 59, 65, 67…. However, when the number of atoms contained in a cluster is more than 70, the position of its magic number would be ambiguous.

In order to further reveal the magic number characteristics of the above-mentioned groups, we show the variation of the numbers of clusters in the system with the numbers of atoms contained in the clusters for ten groups in Figure 10, respectively.

It is observed in Fig.10 that although the ranges of neighboring groups have overlapped each other, one or two partial magic numbers still can be obviously distinguished for each group, and all the partial magic numbers for the ten groups rather correspond to the total magic number sequence for the whole system as shown in Figure 10. Going further, the total magic number sequence can be classified again according to the order of the ten groups of clusters in the following sequence: 13 (first magic number), 19 (second), 25-27(third), 31-33(fourth), 38-40(fifth), 42-45(sixth), 48-51(seventh), 55-59(eighth), 61-65(ninth) and 67(tenth). The ninth and tenth magic numbers are not so obvious in figure 10 because the numbers of clusters containing 9 and 10 basic clusters are insufficient, however, they stand out in figure 10 (c). For simplicity, the magic number sequence corresponding to the order of the ten groups of clusters can be listed again as 13, 19, 25(27), 31(33), 38(40), 42(45), 48(51), 55(59), 61(65) and 67, where the numbers in bracket are the secondary magic numbers of the corresponding groups of clusters. We think the above-mentioned analysis is very important for searching the origin of the magic number of clusters formed in the system.

We compare the total magic number sequence mentioned above to the experimental results of the photo-ionization mass spectra of clusters, formed through supersonic deposition from supersaturated gaseous phase Al, obtained by Schriver et al as shown in Fig.3 of Ref. (Schriver et al., 1990), it can be clearly seen that the magic numbers reported (14, 17, 23, 29, 37, 43, 47, 55, 67…), and those not reported (19, 21, 25, 33, and 39) (they can be clearly seen in the same Fig.3, maybe the authors thought those numbers were not consistent with the magic number rule at that time), are almost all consistent with our magic number sequence (in the error range of ±1). Thus, it can be said that the magic number sequence from our simulation is supported by the experimental results, but their clusters are produced by both different formation processes even though they are of the same element, Al.

In particular, as we further compare the magic number sequence from our simulation to the experimental results of inert gas clusters, it can be also clearly seen that the magic number sequence obtained from the mass spectra of Ar clusters formed in a supersaturated ionic

phase given by Harris et al is 13, 19, 23, 26, 29, 32, 34, 43, 46, 49, 55, 61, 64, 66... (see Fig.1 in Ref. (Harris, Kidwell & Northby, 1984), and the sequence obtained from the mass spectra of Xe clusters formed in a supersaturated vapor phase given by Echt et al (Echt, Sattler & Recknagle, 1981) is 13, 19, 23, 25, 29, 55, 71... (see Fig.1 in this Ref.), these results are also in good agreement with our sequence in the same error range. That is to say that the this simulation result from metal Al is similar to those from inert gases Ar and Xe, and this similarity should reflect in certain degree some essential relations between different elements, especially in different states.

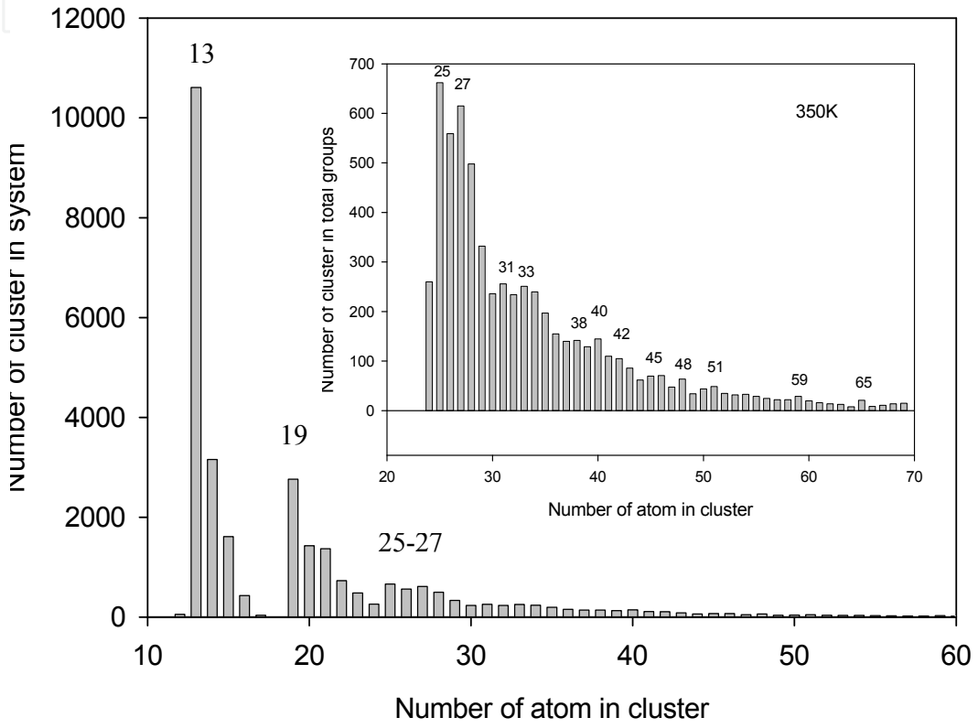

Fig. 9. Variation of the number of clusters in system of Al with sizes of clusters (i. e. the number of atoms contained in the cluster) at 350K.

It is highly interesting that this magic number sequence is also in good agreement with the results, obtained by using MD simulation and other model potentials from Solov'yov's and Doye's works, such as 13, 19, 23, 26, 29, 32, 34, 43, 46, 49, 55, 61, 64, 71, … (see Fig.1 and 2 in Ref. (Solov'yov I A, Solov'yov A V & Greiner, 2003)), and 13, 19, 23, 26, 29, 34, 45, 51, 55,… (see Fig.1 and 2 in Ref. (Doye & Meyer, 2005)) , respectively. From these, it can be explained that as long as the methods used to solve the similar problem are reasonable, the results should also be similar.

4.3.2 Magic number sequence of nana-clusters for liquid metal Na

For liquid metal Na, for deep understanding the size distribution of the clusters mentioned above, we also only analyze ten group levels in the system in turn by the numbers of basic clusters contained in each group level for two cases of liquid state at 573 K and solid state at

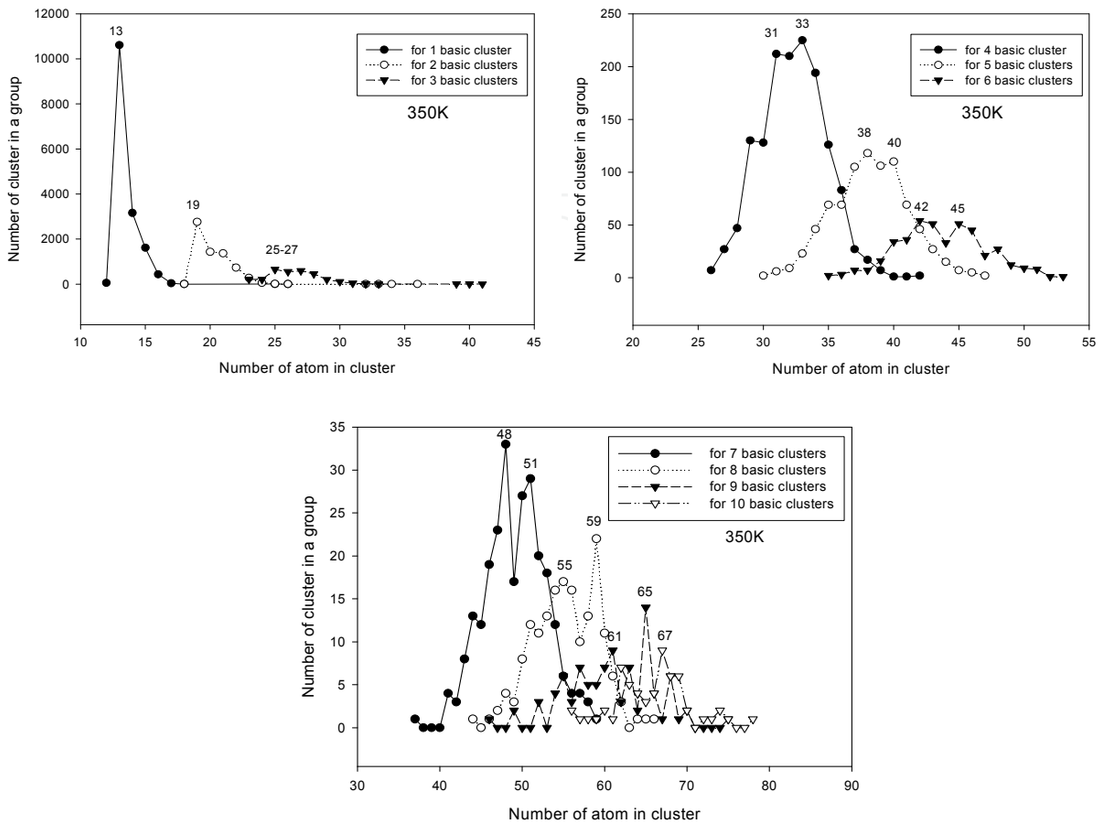

Fig. 10. Relationship of the numbers of basic clusters in a group with the size of cluster (number of atoms contained in a cluster) at 350K in system of Al. (a) for 1 ~ 3 group; (b) for 4 ~ 6 group; (c) for 7 ~ 10 group.

223 K, as shown in Table 6. From Table 6, it can be clearly seen that there is a peak value (maximum) of the numbers of clusters for each group, and this is shown with a short underline in the table. It is also found that the positions of the peak value points of the numbers of clusters are corresponded to the magic number points. In liquid state, the magic numbers are in the order of 14, 21, 28, 34…, and it is not clear for the clusters contained more than five basic clusters. In solid state, the magic numbers are in the order of 14, 22, 28, 34, 41(43), 46(48), 52(54), 57(59), 61(66), 70(74), which are corresponding to the first, second, third, …. and tenth group levels, respectively, the numbers in the brackets are the second magic numbers corresponding to the same group level. The first four magic numbers are almost the same as in liquid state; thereafter, it is also not clear for the clusters contained more than ten basic clusters.

On the other hand, for further understanding the magic number characteristics of the group level of clusters, the relations of the number of clusters in each group level with the number of atoms contained in each cluster for twelve groups, and the total number of clusters in all the group levels enclosed at 223K are shown in Fig 11 (a), (b), (c) and (d).

Cluster consisting of 1 basic clusters		Cluster consisting of 2 basic clusters		Cluster consisting of 3 basic clusters		Cluster consisting of 4 basic clusters		Cluster consisting of 5 basic clusters	
Cluster size	Cluster number	Cluster size	Cluster number	Cluster size	Cluster number	Cluster size	Cluster number	Cluster size	Cluster number
Number of atom	573K 223K	Number of atom	573K223K	Number of atom	573K223K	Number of atom	573K223K	Number of atom	573K223K
10	2 0	17	3 0	23	0 5	28	0 7	32	0 1
11	43 4	18	9 8	24	2 28	29	0 21	33	0 6
12	297 149	19	46 227	25	15 108	30	2 54	34	0 17
13	1180 2771	20	133 788	26	18 369	31	4 131	35	2 26
14	**1650** **5962**	**21**	**213** 1736	27	26 620	32	1 193	36	0 66
15	1119 4992	**22**	182 **1883**	**28**	**36 708**	33	4 271	37	1 92
16	412 1404	23	102 1167	29	25 638	**34**	**6 334**	38	1 120
17	59 151	24	46 507	30	19 503	35	4 322	39	0 156
18	6 0	25	9 134	31	12 305	36	5 284	40	1 162
		26	2 22	32	4 138	37	3 239	**41**	**0 179**
		27	0 3	33	2 47	38	1 153	42	0 164
				34	0 11	39	1 84	43	0 154
						40	0 36	44	1 105
						41	0 17	45	1 68
						42	0 1	46	0 51
						43	0 1	47	0 24
								48	0 10
								49	0 4
								50	0 1

(continued)

Cluster consisting of 6 basic clusters		Cluster consisting of 7 basic clusters		Cluster consisting of 8 basic clusters		Cluster consisting of 9 basic clusters		Cluster consisting of 10 basicclusters	
Cluster size	Cluster number	Cluster size	Cluster number	Cluster size	Cluster number	Cluster size	Cluster number	Cluster size	Cluster number
Number of atom	573K 223K	Number of atom	573K223K	Number of atom	573K223K	Number of atom	573K223K	Number of atom	573K223K
38	0 6	41	0 1	44	0 1	51	0 3	53	0 1
39	0 19	42	0 3	45	0 0	52	0 2	54	0 0
40	0 24	43	0 4	46	0 3	53	0 4	55	0 2
41	0 29	44	0 2	47	0 4	54	0 7	56	0 2
42	1 59	45	1 16	48	0 8	55	0 15	57	0 5
43	2 79	46	0 38	49	0 6	56	0 11	58	0 5
44	0 96	47	0 40	50	1 21	57	0 15	59	0 5
45	0 **114**	48	0 60	51	0 17	58	0 27	60	0 10
46	1 **114**	49	0 54	52	0 30	**59**	1 **34**	61	0 14
47	0 97	50	0 50	53	0 38	60	0 31	62	0 7
48	0 **107**	**51**	0 **65**	**54**	0 **54**	**61**	0 **34**	63	0 14
49	1 98	**52**	0 **66**	55	0 36	62	0 34	64	0 17
50	1 73	53	0 56	56	0 41	63	0 32	65	0 20
51	0 44	54	0 63	**57**	0 **50**	64	0 20	**66**	**0 23**
52	0 33	**55**	0 **65**	58	0 45	65	0 32	67	0 18
53	0 23	56	0 42	**59**	0 **50**	**66**	0 **39**	68	0 25
54	0 20	57	0 42	60	0 41	67	0 26	69	0 23
55	0 10	58	0 36	61	0 42	68	0 23	**70**	**0 26**
56	0 2	59	0 26	62	0 39	69	0 17	71	0 21
57	0 1	60	0 18	63	0 25	**70**	0 22	72	0 19
		61	0 11	64	0 19	71	0 15	73	0 21
		62	0 11	65	0 17	72	0 14	**74**	**0 22**
		63	0 1	66	0 10	73	0 12	75	0 21
		64	0 1	67	0 4	74	0 6	76	0 8
				68	0 1	75	0 1	77	0 8
				69	0 5	76	0 1	78	0 8
				70	0 2	77	0 2	79	0 5
								80	0 8
								81	0 5

Table 6. Relations of the number of clusters consisting of 1-10 basic clusters with the cluster size (number of atoms included) for liquid metal Na.

Highly interesting is that though the ranges of neighboring group levels are overlapped each other as shown in Fig 11, the magic number of each group level is still clearly corresponded to the magic number of the total magic number sequence for all the group

levels at the same group level. For this point, as we consider the magic number of each group level as the corresponding partial magic number, the total magic number sequence of all the group levels can be considered as the superposition of all the partial magic numbers.

Therefore, the total magic number sequence can be analyzed according to the corresponding group level in the order of 14(the first magic number), 22(second), 28(third), 34(fourth), 41-43(fifth), 46-48(sixth), 52-54 (seventh), 57-59(eighth), 61-66(ninth) and 70-74(tenth). However, the last three magic numbers also cannot be clearly distinguished in the Fig.11 (d), since the numbers of the larger clusters containing more basic clusters are not enough.

Going further, it can be seen that not only have the experimental results reported by Schriver and Harris et al (Schriver et al., 1990; Harris, Kidwell & Northby, 1984) provided a vital experimental certification to our simulation results, but also our simulation results could provide a reasonable model explanation to those experimental results. As regards the magic numbers obtained from experimental researches, some of them can be explained as usual with the viewpoint of geometric shell structure of cluster configurations being closed regularly (for neutral clusters and charged clusters) (Knight et.al., 1984; Harris et al., 1984; Echt, Sattler & Recknagle, 1981; Schriver et al., 1990; Robles, Longo & Vega, 2002), and the others cannot be explained with the same viewpoint because they are corresponding to the geometric non-shell structure of cluster configurations. However, from our simulation, it can be clearly seen that during the forming process of larger clusters, only a few clusters accumulate and extend continuously with a basic cluster as the core according to a certain rule; most of them are formed with combining different numbers and different types of basic clusters. So, it is the normal case and can be explained to find more clusters with geometric non-shell structure in their magic number sequence as above-noted.

So far, the critical question is why the magic number sequence of clusters formed by solidification of liquid metal Al from our simulation is so similar to those magic number sequences of clusters formed by ionic spray and gaseous deposition of metal Al, inert gases Ar and Xe from experimental studies? We think the main reason is that the solidification process of liquid metal is essentially similar to the formation process of clusters in the above-mentioned experimental studies. We consider that in the solidification process of liquid metals, various cluster configurations could be formed by the rapid agglomerating of a large number of atoms as the system spreads over a large space for a short time, while in the formation process of clusters in the experiments, various cluster configurations could be formed by slow gathering of a few atoms as the system spreads over a small space for a long time, and both their final results could be similar each other on the whole (even though they are not be similar completely). On the other hand, at present, the essential differences between different elements, especially different states, are still not be distinguished in detail, it is necessary to analyze and compare in detail various similar and dissimilar magic numbers of these sequences in the future.

Therefore, it may be feasible to adopt magic numbers, especially the partial magic numbers of the group levels, obtained during the rapid solidification process of liquid metals to understand the magic number characteristics obtained with experimental methods.

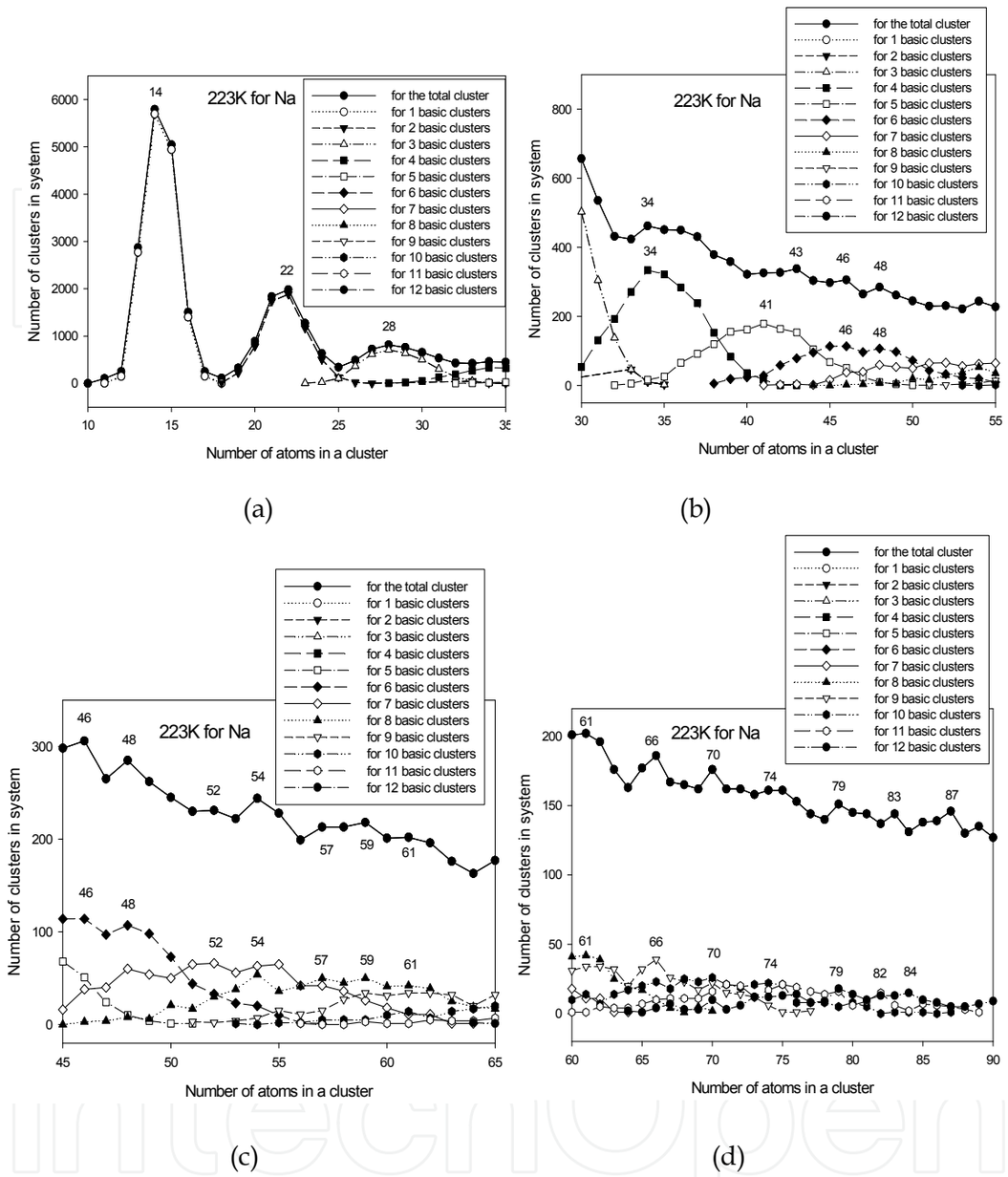

Fig. 11. Relations of the number of cluster in a group with the size of cluster (i. e. atoms included in cluster) at 223K .(a) for 1 ~ 3 groups; (b) for 4 ~ 6 groups; (c) for 7 ~ 9 groups; (d) for 10 ~ 12 group levels of clusters .

4.3.3 Stability of nana-clusters

From the above mentioned, it can be clearly seen that the larger clusters within a same group level should have not the same number of atoms because they contained different basic clusters containing different number of atoms. Therefore, these larger clusters would have different number of atoms. It can be clearly seen that those larger clusters containing

minority of atoms in which the central atoms of basic clusters are connected tightly each other with multi-bonded, would be more stable than others and they would possess better stability and higher heredity, and so on.

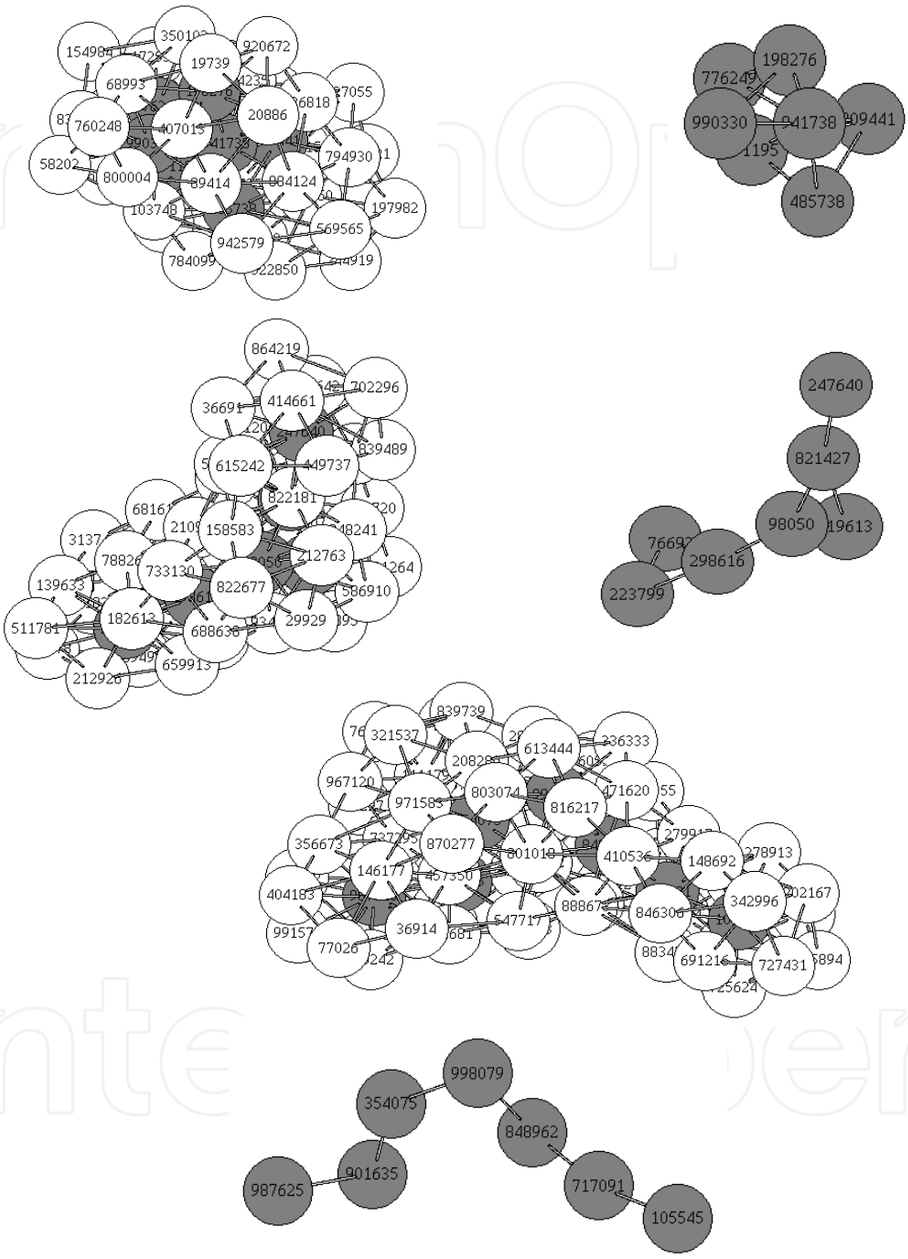

Fig. 12. Schematic diagram of three larger clusters consisting of 43, 53 and 69 atoms within 7 basic clusters with connecting bonds, respectively, at 223K (the gray spheres are the center atoms of basic clusters).

These features can be shown in Fig.12. It is the schematic diagram of three larger clusters consisting of 43, 53 and 69 atoms within the same group level of 7 basic clusters, with

connecting bonds, respectively, at 223K (the gray spheres are the center atoms of basic clusters). From the diagrams of their center atoms with multi-bonded or single-bonded each other, it can be clearly seen that the cluster consisting of 43 atoms has a dense connecting of all atoms and would possess better stability and higher heredity than other two clusters consisting of 53 and 69 atoms, respectively, in turn.

5. Conclusions

In this chapter, for deeply understanding the formation and evolution characteristics of various clusters, especial of nano-clusters formed during solidification processes, molecular dynamic simulation studies have been performed for a large-sized system consisting of 10^6 liquid metal for Al and Na atoms, respectively. Several microstructure analysis methods, especial the cluster-type index method (CTIM) have been adopted to describe various types of cluster, especial of nano-cluster by basic clusters. It is demonstrated that the icosahedral cluster (12 0 12 0) is the most important basic cluster, and plays a critical role in the microstructure transition. The nano-clusters are formed by connecting various middle and small clusters with different cluster-types or sizes, and their structures are different from those obtained by gaseous deposition, ionic spray and so on.

For the evolution processes of the nano-clusters, at different temperatures, it is demanstrated clearly that the central atoms of basic clusters in the nano-clusters are bonded each other with different ways, some central atoms are multi-bonded, and others single-bonded. A new statistical method has been proposed to classify the clusters (from basic cluster to nano-cluster) formed in the system by the number of basic cluster contained in them, and the clusters consisting of the same number of basic cluster but not the same number of atoms can be classified as a group level of clusters. It can be clearly seen that the size distribution characteristics of various clusters in the system is related to the magic number of each group level of clusters. The total magic number sequence of the system can be obtained for metal Al as 13, 19, 25(27), 31(33), 38(40), 42(45), 48(51), 55(59), 61(65) , 67, ... the numbers in the brackets are the second magic numbers corresponding to the same group level of clusters. This magic number sequence is in good agreement with the experimental results obtained by Schriver and Harris et al (for Al). For metal Na, the magic number sequence are in the order of 14, 22, 28, 34, 41(43), 46(48), 52(54), 57(59), 61(66), 70(74), …This magic number sequence is in good agreement with the experimental results obtained by Knight et al and the calculating results obtained by Noya et al (containing the primary and secondary magic numbers) (for Na). Highly interesting, these simulation results can be used to provide a reasonable explanation for those experimental results.

6. Acknowledgment

This work was supported by the National Natural Science foundation of China (Grant No 50831003, 50571037)

7. References

Alexander, V. M. & Moshe, B. Z., (2001). Temporal evolution of an argon cluster during the process of its evaporation, *Chemical Physics*, Vol. 264: 135−143.

Alfe, D. (2003). First-principles simulations of direct coexistence of solid and liquid aluminum, *Phys. Rev. B* , Vol. 68: 064423.

Bruhl, R., Guardiola, R., Kalinin, A., et al., (2004) Diffraction of Neutral Helium Clusters: Evidence for "Magic Numbers", *Phys. Rev. Lett.* , Vol.92: 185301.

Cabarcos, O. M. & Lisy, J. M. (1999). Molecular dynamics simulation of gas phase ion cluster formation, *International Journal of Mass Spectrometry,* Vol. 185/186/187: 883-903.

Dong, K. J., Liu, R. S., Yu, A. B., et al., (2003). Simulation study of the evolution mechanisms of clusters in a large-scale liquid Al system during rapid cooling processes, *J. Phys. : Condens. Matter,* Vol. 15: 743-753.

Doye, J. P. K. & Meyer, L. (2005). Mapping the Magic Numbers in Binary Lennard-Jones Clusters，*Phys. Rev. Lett.*, Vol. 95: 063401.

Echt, O., Sattler, K. & Recknagle, E. (1981). Magic numbers for sphere packings: Experimental verification in free xe-non clusters，*Phys. Rev. Lett.,* Vol.47: 1121-1124.

Evans, D. J. (1983). Computer ''experiment'' for nonlinear thermodynamics of Couette flow, *J. Chem. Phys.,* Vol. 78: 3297-3302.

Kostko, O., Huber, B., Moseler, M., et al., (2007). Structure determination of medium-sized sodium clusters, *Phys. Rev. Lett.,* Vol. 98: 043401.

Knight, W. D., Clemenger, K., de Heer, W. A., et al., (1984). Electronic shell structure and abundances of sodium clusters, *Phys. Rev. Lett.,* Vol. 52: 2141-2143.

Harris, I. A., Kidwell, R. S. & Northby, J. A. (1984). Structure of charged argon clusters formed in a jet expansion, *Phys. Rev. Lett.,* Vol.53: 2390—2393.

Haberland, H., Hippler, T., Donges, J., et al., (2005). Melting of sodium clusters: where do the magic numbers come from?, *Phys. Rev. Lett.,* Vol. 94: 035701

Honeycutt, J. D. & Andersen, H. C. (1987). Molecular-dynamics study of melting and freezing of small Lennard-Jones, *J. Phys Chem.,* Vol. 91: 4950-4963.

Hoover, W. G., Ladd, A. J. C. & Moran, B. (1982). High-strain-rate plastic flow studied via nonequilibrium molecular dynamics, *Phys. Rev. Lett.,* Vol. 48: 1818.-1820

Hou, Z. Y., Liu, L. X., Liu, R. S., et al., (2009). Simulation study on the evolution of thermodynamic, structural and dynamic properties during the crystallization process of liquid Na, *Modelling Simul. Mater. Sci. Eng*, Vol. 17 : 035001.

Hou, Z. Y., Liu, L. X., Liu, R. S., et al., (2010a) Short-range and medium-range order in Ca7Mg3 metallic glass, *J Appl. Phys.*, Vol. 107: 083511

Hou, Z. Y., Liu, L. X., Liu, R. S., et al., (2010b). Kinetic details of nucleation in supercooled liquid Na: A simulation tracing study, *Chemical Physics Letters*, Vol. 491: 172-176

Ikeshoji, T., Hafskjold, B., Hashi, Y., et al., (1996). Molecular Dynamics Simulation for the Formation of Magic-Number Clusters with a Lennard-Jones Potential，*Phys. Rev. Lett.* , Vol. 76: 1792-1795.

Joshi, K., Krishnamurty, S. & Kanhere, D. G.,(2006), "Magic melters" have geometrical origin, *Phys. Rev. Lett.,* Vol. 96 : 135703

Kostko, O., Huber, B., Moseler, M., et al., (2007). Structure determination of medium-sized sodium clusters, *Phys. Rev. Lett.,* Vol. 98: 043401.

Li, D. H., Li, X. R. & Wang, S. (1986). Variational calculation of helmholtz free energies with applications to the sp-type liquid metals, *J. Phys F,* Vol. 16: 309-321.

Li, H. & Pederiva, F. (2003). Anomalies in liquid structure of Ni_3Al alloys during a rapid cooling process, *Phys. Rev. B*, Vol. 68: 054210

Liu, C. S., Zhu, Z. G., Xia, J. C., et al., (2001). Cooling rate dependence of structural properties of aluminium during rapid solidification, *J. Phys.:Condens. Matter,* Vol. 13 : 1873-1890.

Liu, F. X., Liu, R. S., Hou, Z. Y., et al., (2009). Formation mechanism of atomic cluster structures in Al-Mg alloy during rapid solidification processes, *Annals of Physics*， Vol. 324 : 332–342.

Liu, R. S., Qi, D. W. & Wang, S. (1992a). Subpeaks of structure factors for rapidly quenched metals, *Phys. Rev. B,* Vol. 45: 451-453.

Liu, R. S. & Wang S. (1992b). Anomalies in the structure factor for some rapidly quenched metals, *Phys. Rev. B*, Vol. 46:12001-12003.

Liu, R. S., Li, J. Y. & Zhou, Q. Y. (1995). A simulation study on the transition feature of the microstructure in the forming process of amorphous metals, *Chinese Science Bulletin*, Vol. 40: 1429-1433.

Liu, R. S., Li, J. Y., *et al.*, (1998). The stability of microstructures during rapid cooling processes of Al liquid metal, *Trans. Nonferrous Met. Soc. China,* Vol. 8: 533—538.

Liu, R. S., Li, J. Y., Zhou, Z., et al., (1999) The high-temperature properties of the micro-structure transition in liquid metals, *Mater. Sci. Eng. B,* Vol. 57: 214-217.

Liu, R. S., Li, J. Y., Dong, K. J., et al., (2002). Formation and evolution properties of clusters in a large liquid metal system during rapid cooling processes, *Mater. Sci. Eng. B,* Vol. 94:141-148.

Liu, R. S., Dong, K. J., Li, J. Y.,et al., (2005a). Formation and description of nano-clusters formed during rapid solidification processes in liquid metals , *J. Non-Cryst. Solids,* Vol. 351: 612-617.

Liu, R. S., Dong, K. J., Liu, F. X., et al., (2005b). Formation and evolution mechanisms of large-clusters during rapid solidification process of liquid metal A1, *Science in China (Series G),* Vol. 48: 101-112.

Liu, R. S., Liu, F. X., Zhou, Q. Y., (2007a). Formation and magic number characteristics of cluster configurations during rapid cooling processes of liquid metals, in Editor(s): Bai, C., et al,. *Nanoscience and Technology, Pts 1 and 2* of Book Series: *Solid State Phenomena,* Vol. 121-123 pp: 1139-1142.

Liu, R. S., Tian, Z. A., Yi, X. H., et al., (2007b). Evolution mechanisms of nano-clusters in a large-scale system of 10(6) liquid metal atoms during rapid cooling processes, in Editor(s): Bai, C., et al,. *Nanoscience and Technology, Pts 1 and 2* of Book Series: *Solid State Phenomena,* Vol. 121-123 pp: 1049-1052.

Liu, R. S., Dong, K. J., Tian, Z. A., et al., (2007c). Formation and magic number characteristics of clusters formed during solidification processes, *J. Phys.:Condens. Matter*, Vol.19: 196103.

Liu, R. S., Liu, H. R., Dong, K. J., et al., (2009). Simulation study of size distributions and magic number sequences of clusters during the solidification process in liquid metal Na, *J. Non-Cryst. Solids*， Vol. 355: 541-547.

Liu, X. H., Zhang, X. G., Li, Y. *et al.*, (1998). Cluster formation by direct laser vaporization: Evidence for the twofold mechanism, *Chem. Phys. Lett.*, Vol. 288: 804—808.

Magudoapathy, P., Gangopadhyay, P., Panigrahi, B. K., et al., (2001). Electrical transport of Ag nanoclusters embedded in glass matrix, *Physica B,* Vol.299: 142-146.

Martin, T. P., Naher, U. & Schaber, H. (1992). Evidence for octahedral shell structure in aluminum clusters, *Chem. Phys. Lett.,* Vol. 199: 470-474.

Noya, E.G., Doye, J.P.K., Wales, D.J., et al., (2007). Geometric magic numbers of sodium clusters: Interpretation of the melting behaviour, *Eur. Phys. J. D*, Vol. 43: 57-60.

Orlando, M. C. & James, M. L., (1999). Molecular dynamics simulation of gas phase ion cluster formation, *International Journal of Mass Spectrometry*, Vol. 185/186/187: 883 - 903.

Qi, D. W. & Wang, S. (1991a). Thermodynamic calculations for glasses: thermodynamic properties of the metallic glass transition, *J. Non-Cryst. Solids,* Vol. 135: 73-78.

Qi, D. W. & Wang, S. (1991b). Icosahedral order and defects in metallic liquids and glasses, *Phys Rev. B,* Vol. 44 : 884-887.

Robles, R., Longo, R. C. & Vega, A. (2002). Magnetic magic numbers are nt magic for clusters embedded in noble metals, *Phys. Rev. B,* Vol. 66: 064410.

Schriver, K. E., Person, J. L., Honea, E. C., et al., (1990). Electronic shell structure of group-IIIA metal atom clusters, *Phys. Rev. Lett.* , Vol. 64: 2539-2542.

Solov'yov, I. A., Solov'yov, A. V. & Greiner, W. (2003). Cluster growing process and a sequence of magic numbers, *Phys. Rev. Lett.* , Vol. 90: 053401.

Spiridis, N., Haber, J. & Korecki, J. (2001). STM studies of Au nano-clusters on TiO_2(1 1 0) , *Vacuum,* Vol. 63: 99-105.

Tian, Z. A., Liu, R. S., Zheng, C. X., et al., (2008). Formation and Evolution of Metastable bcc Phase during Solidification of Liquid Ag: A Molecular Dynamics Simulation Study, J. Phys. Chem. A, Vol. 112 : 12326.

Tian, Z. A., Liu, R. S., Peng, P., et al., (2009). Freezing structures of free silver nanodrplets: A moleculart dynamics simulation study, *Phys. Lett. A,* Vol. 373: 1667-1671.

Wang, L., Bian, X. F. & Zhang, J. X. (2002). Structural simulation of clusters in liquid Ni50Al50 alloys, *Modelling Simul. Mater. Sci. Eng.* ,Vol. 10: 331-339

Wang, S. & Lai, S. K. (1980). Structure and electrical resistivities of liquid binary alloys, *J. Phys F,* Vol. 10: 2717-2737.

Waseda, Y. (1980). *The structure of Non-crystalline Materials* (New York: McGraw-Hill), p. 270.

Wendt, H. R. & Abraham, F. F. (1978). Empirical criterion for the glass transition region based on Monte Carlo simula-tions, *Phys. Rev. Lett.,* Vol. 41: 1244-1246.

Yamamoto, H. & Asaoka, H. (2001). Formation of binary clusters by molecular ion irradiation, *Appl. Surf. Sci.,* Vol.169-170: 305-309.

Zheng, C. X., Liu, R. S., *et al.*,(2002). Simulation study on the formation and transition properties of cluster structures in liquid metals during rapid cooling processes, *Science in China, Series A,* Vol. 45(2): 233—240.

Zhou, L. L., Liu, R. S., Tian, Z. A., et al.,(2011). Formation and evolution characteristics of bcc phase during isothermal relaxation processes of supercooled liquid and amorphous metal Pb, *Trans. Nonferrous Met. Soc. China,* Vol. 21: 588-597.

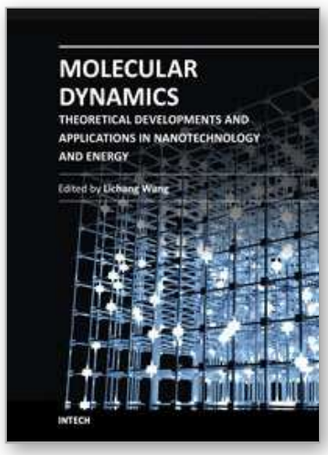

Molecular Dynamics - Theoretical Developments and Applications in Nanotechnology and Energy

Edited by Prof. Lichang Wang

ISBN 978-953-51-0443-8
Hard cover, 424 pages
Publisher InTech
Published online 05, April, 2012
Published in print edition April, 2012

Molecular Dynamics is a two-volume compendium of the ever-growing applications of molecular dynamics simulations to solve a wider range of scientific and engineering challenges. The contents illustrate the rapid progress on molecular dynamics simulations in many fields of science and technology, such as nanotechnology, energy research, and biology, due to the advances of new dynamics theories and the extraordinary power of today's computers. This first book begins with a general description of underlying theories of molecular dynamics simulations and provides extensive coverage of molecular dynamics simulations in nanotechnology and energy. Coverage of this book includes: Recent advances of molecular dynamics theory Formation and evolution of nanoparticles of up to 106 atoms Diffusion and dissociation of gas and liquid molecules on silicon, metal, or metal organic frameworks Conductivity of ionic species in solid oxides Ion solvation in liquid mixtures Nuclear structures

INTECH
open science | open minds

InTech Europe
University Campus STeP Ri
Slavka Krautzeka 83/A
51000 Rijeka, Croatia
Phone: +385 (51) 770 447
Fax: +385 (51) 686 166
www.intechopen.com

InTech China
Unit 405, Office Block, Hotel Equatorial Shanghai
No.65, Yan An Road (West), Shanghai, 200040, China
中国上海市延安西路65号上海国际贵都大饭店办公楼405单元
Phone: +86-21-62489820
Fax: +86-21-62489821

IntechOpen